Crystal-field and charge transfer transitions due to Cr 3+ ions in fluorides

J. A. Aramburu, M. Moreno, K. Doclo, C. Daul, and M. T. Barriuso

Citation: The Journal of Chemical Physics **110**, 1497 (1999); doi: 10.1063/1.478023
View online: http://dx.doi.org/10.1063/1.478023
View Table of Contents: http://scitation.aip.org/content/aip/journal/jcp/110/3?ver=pdfcov
Published by the AIP Publishing

Crystal-field and charge transfer transitions due to Cr^{3+} ions in fluorides

J. A. Aramburu and M. Moreno
Departamento Ciencias de la Tierra y Física de la Materia Condensada, Facultad de Ciencias, Universidad de Cantabria, E-39005 Santander, Spain

K. Doclo and C. Daul
Institut de Chimie Inorganique et Analytique, Université de Fribourg, CH 1700 Fribourg, Switzerland

M. T. Barriuso
Departamento Física Moderna, Facultad de Ciencias, Universidad de Cantabria, E-39005 Santander, Spain

(Received 23 April 1998; accepted 7 October 1998)

The metal-ligand equilibrium distance, R_e, vibrational frequencies, crystal-field (CF) and charge transfer (CT) transition energies, Huang–Rhys factors, Stokes shift, as well as oscillator strengths of allowed CT transitions due to Cr^{3+} in fluorides, have been investigated using density functional theory. CrF_6^{3-} and $CrF_6K_8K_6^{11+}$ clusters simulating Cr^{3+} in the K_3CrF_6 lattice have been used. In the $CrF_6K_8K_6^{11+}$ cluster the computed equilibrium distance using a generalized gradient approximation functional is $R_e=1.88$ Å and an overall agreement with experimental spectroscopic parameters is achieved. As salient feature it is pointed out that 6% errors in R_e can lead to errors of ~40% and ~25%, respectively, in the calculated vibrational frequencies and the 10 Dq parameter. Moreover the force constant, k_T, involved in the A_{1g} symmetrical mode at the equilibrium distance is shown to be mainly determined by the interaction between the central ion and the ligands while the interaction between the latter ones and K^+ neighbors leads to a contribution which is about 25% of k_T. The calculated oscillator strengths confirm that the transitions involving the ligand t_{1u} orbital and the antibonding $e_g^*\uparrow$ and $e_g^*\downarrow$ ones should be the most intense among the nine allowed CT transitions. Moreover, CT transitions connecting two orbitals which do not have the same σ or π character are found to display an oscillator strength much smaller than for the rest of the cases. This idea is shown to be also valid for other transition-metal complexes. The computed Huang–Rhys factor associated with the A_{1g} mode, S_A, for the lowest CT transition is shown to be about ten times higher than that corresponding to the $^4T_{2g}$ CF state and explains the experimental bandwidth. The origin of this important difference is discussed. Finally, the electronic relaxation in the first $^4T_{2u}$ CT state is shown to induce an important decrement (~40%) of the $^4A_{2g}\rightarrow{}^4T_{2u}$ transition energy and an increase of the total charge on the central ion of only 0.2 *e*. © *1999 American Institute of Physics.* [S0021-9606(99)30602-4]

I. INTRODUCTION

A great deal of experimental work has been focused on the optical properties due to sixfold coordinated Cr^{3+} ions in different fluoride lattices.[1–15] That research has been stimulated by the application of some of those systems in fields such as broad band solid state lasers[16] or thermometry.[17]

In parallel to that investigation theoretical calculations have also been carried out for explaining the microscopic origin of absorption and emission spectra due to CrF_6^{3-} units embedded in different fluorides.[18–27] Nevertheless this research has practically been devoted to analyse the parity forbidden crystal-field (CF) excitations while little attention[27] has been paid to the allowed charge transfer (CT) excitations. Though for $3d$ ions the latter transition usually lie at higher energies than the former ones, the allowed CT transitions are however responsible for the polarizability of a chromophore like CrF_6^{3-}. Owing to this fact, the Raman scattering due to a transition-metal complex is substantially enhanced as far as the energy of the incident light becomes closer to that corresponding for CT transitions.[28,29] On the other hand, a detailed knowledge about these transitions is also important as regards the optical absorption processes in the first excited state. Although it is expected[1] that the lowest CT transition energy for CrF_6^{3-} lies just a little above the limit of the optical range ($E_e=6.5$ eV) experimental information about CT transitions in $Na_3In_2Li_3F_{12}:Cr^{3+}$ has however been reported.[10] In fact the excitation spectra of the $^4T_{2g}\rightarrow{}^4A_{2g}$ emission has been observed up to photon energies of 30 eV using synchrotron radiation whose main results are summarized in Fig. 1.

Up to now however these attractive experimental data have only been explored by means of multiple scattering-$X\alpha$ (MS-$X\alpha$) and self-consistent charge extended Hückel (SCCEH) calculations on simple CrF_6^{3-} units performed at and around the experimental equilibrium Cr^{3+}–F^- distance corresponding to the $^4A_{2g}$ ($(t_{2g}^*)^3$ configuration) ground state.[27] By contrast none of Hartree–Fock calculations carried out on CrF_6^{3-} in fluorides[18–21,23–25] has explored the CT transitions. It is worth noting that in some Hartree–Fock calculations the mainly $2p$(F) levels have been found to be close to the $3d$ levels of the central Cr^{3+} ion.[23] Although the MS-$X\alpha$ and SCCEH calculations on CrF_6^{3-} both support the

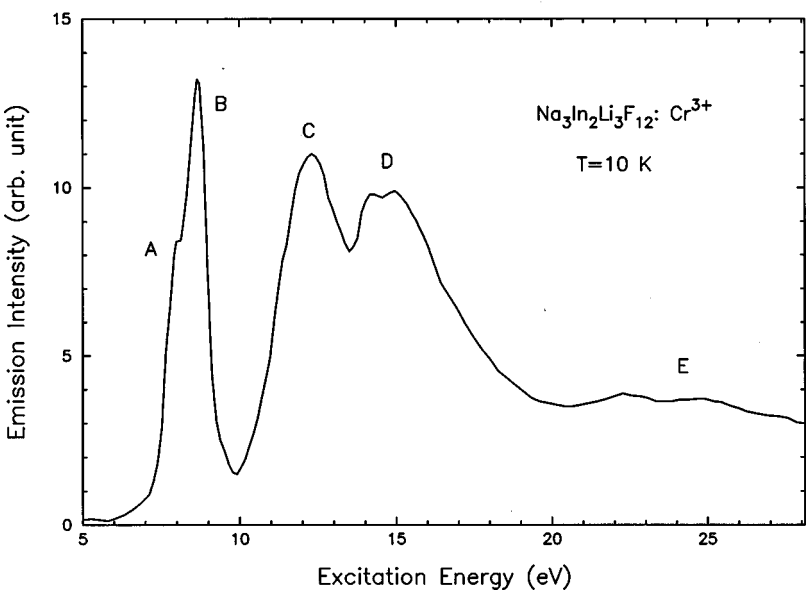

FIG. 1. Excitation spectrum of $Na_3In_2Li_3F_{12}:Cr^{3+}$ in the 5–30 eV range measured (Ref. 9) at $T=10$ K. The present figure is taken from Ref. 27.

assignment of bands *A*, *B*, and *C* of Fig. 1 as CT transitions,[27] an important problem is raised concerning the number of observed CT bands. In fact the allowed CT transitions in CrF_6^{3-} correspond to jumps denoted as $(\gamma_L)^6(t_{2g}^*)^3 \rightarrow (\gamma_L)^5(t_{2g}^*)^m(e_g^*)^n(S')$. Here γ_L can be one of the two t_{1u} bonding orbitals or the t_{2u} nonbonding one while S' denotes the spin of the $3d$ subshell[1,27] formed by all the electrons placed in the antibonding t_{2g}^* and e_g^* orbitals. As regards the values of m and n there are two possibilities, either $m=4$, $n=0$, and $S'=1$ or $m=3$, $n=1$, and then $S'=2$ or $S'=1$. Therefore neglecting spin–orbit coupling a total of nine CT transitions are allowed.

Bearing in mind the results on $CuCl_4^{2-}$ units[30] it was proposed tentatively[27] that CT jumps where the initial and final level both exhibit some σ-character, possess a higher oscillator strength than the other transitions. In other words, peaks A and B of Fig. 1 were assigned to the $t_{1u}(\sigma-\pi)\uparrow \rightarrow e_g^*\uparrow$ and $t_{1u}(\sigma+\pi)\uparrow \rightarrow e_g^*\uparrow$ one-electron transitions, respectively. In the level called $t_{1u}(\sigma-\pi)(t_{1u}(\sigma+\pi))$ the σ and π combinations of ligand $2p$(F) orbitals lead to a decrement (increase) of electronic density in the region between two adjacent ligands, and so it has an antibonding (bonding) character with respect to the ligand–ligand interaction. Following this idea, band *C* was assumed to be formed by the two unresolved $t_{1u}(p)\uparrow \rightarrow e_g^*\uparrow$ $(p=\sigma-\pi;\sigma+\pi)$ transitions. For supporting the referred tentative explanation of Fig. 1, it is however fully necessary to calculate the oscillator strength of the nine allowed CT transitions.

This work is primarily devoted to gain a better insight into the CT and CF excitations due to Cr^{3+} impurities in fluorides. For achieving this goal, the density functional theory (DFT) as implemented in the Amsterdam Density Functional (ADF) code has been used.[31,32] Recently DFT calculations[33] on CrX_6^{3-} units (X=Cl, Br) using the multiplet description by Daul *et al.*[34,35] has offered a reasonable description of CF states due to Cr^{3+} in chloro- and bromoelpasolites. Also ADF calculations on $Cr(CO)_6$ have recently clarified[36] the photodissociation mechanism and the role played by CT states in this molecule.

In the present work, besides the calculations of CF multiplets and CT energies, the oscillator strength of the nine allowed CT excitations has been computed using the ADF and also the MS-$X\alpha$ framework. As 10 Dq-dependent CF transitions[22,23] as well as CT excitations[27] appear to be rather sensitive to changes of the metal-ligand distance, *R*, it is crucial to reproduce the experimental equilibrium distance, R_e, corresponding to CrF_6^{3-} units in fluorides, which is found to be very close to 1.90 Å.[37] Owing to this fact aside from CrF_6^{3-} simple units, we have studied the 21 atoms cluster $CrF_6K_8K_6^{11+}$ and the influence of the Madelung potential due to the rest of the K_3CrF_6 lattice. It will be seen that the inclusion of further neighbor ions in the cluster leads to R_e values practically coincident with experiment. Furthermore parameters like vibrational frequencies, the $^4A_{2g} \rightarrow {}^4T_{2g}$ transition energy or the Stokes shift, which are all computed at the calculated equilibrium distance, become also closer to experimental ones in the 21 atom cluster.

Finally a particular attention will be addressed to the problem of electronic relaxation in CT excited states. It was early pointed out by Ziegler *et al.*,[38] through discrete variational $X\alpha$ calculations on tretraoxo $d^n(n=0,1,2)$ complexes, that no net transfer of charge exists in those states but an important rearrangement of electronic density. Johansen[39] and more recently Stückl *et al.*[40] have confirmed this conclusion. Through this work we are *also* interested in quantifying how that electronic relaxation modifies the energy of CT transitions, a relevant question which up to now has not been explored.

II. THEORY

A. Calculational methods

All DFT calculations were performed using the ADF program package.[31,32] The approximate self-consistent field

(SCF) Kohn–Sham (KS) one-electron equations are solved by employing an expansion of the molecular orbitals in a basis set of Slater-type orbitals (STO's). All atoms were described through triple-ζ STO basis sets given in the program database and the core electrons ($1s-3p$ for Cr and K, $1s$ for F) were kept frozen.

The local density approximation (LDA) exchange-correlation energy was computed according to Vosko, Wilk, and Nusair's (VWN) parametrization of electron gas data.[41] In the case of generalized gradient approximation (GGA) calculations, we opted for the Becke–Perdew (BP) functional, which uses Becke's[42] gradient correction to the local expression of the exchange energy and Perdew's[43] gradient correction to the local expression of the correlation energy.

The ADF program allows one to introduce an external electric field generated by point charges. Therefore for introducing the Madelung electrostatic potential due to the rest of the K_3CrF_6 lattice (out of the analyzed cluster) the following procedure has been employed. In a first step it has been calculated that potential using Ewald's method in about 1000 points inside a sphere bigger than the cluster. For instance for the $CrF_6K_8K_6^{11+}$ cluster, where the distance between Cr^{3+} and furthest K^+ ions is 4.27 Å, the radius of the sphere has been taken equal to 5.5 Å. For calculating this potential charges on Cr, K, and F ions were assumed to be equal to $+3e$, $+1e$, and $-1e$, respectively. In a second step the potential inside the sphere has been reproduced using about 100 fictitious charges lying outside the sphere. These charges are located at lattice positions although the value of charges itself is fitted in order to reproduce the right potential inside the sphere. Finally these fictitious charges were placed into the ADF calculations.

Geometry optimizations were performed through spin-unrestricted calculations for several states of the clusters, varying only the metal-ligand distance. In the $CrF_6K_8K_6^{11+}$ clusters all K atoms are fixed at the experimental positions corresponding to the K_3CrF_6 lattice.

B. Crystal-field multiplet splitting

In the calculation of the CF multiplet splitting, we follow essentially the method proposed by Ziegler *et al.*[44] According to their results, it is possible to replace the energy of a single determinant (SD) by its corresponding statistical energy as obtained in a DFT calculation. In general, it is not possible to express the energy of a multiplet in function of the energy of one SD. However, it is possible to exploit fully the symmetry in order to simplify the relation between the multiplet splitting and the SD energies. A detailed description of the symmetry reduction of the problem was recently given by Daul.[34] In general, we can write the multiplet wave function as

$$\Psi_k = |\alpha \Gamma m_\Gamma S m_s\rangle, \tag{1}$$

where Γ and S denote the space and spin part of the wave function, respectively, and m_Γ and m_s denote its component in case of degeneracy. The relation between multiplet energies, $E(\Psi_k)$, and the energies of the nonredundant SD's, $E(\phi_{\mu j})$, is given by

$$E(\Psi_k) = \sum_j F_{kj} E(\phi_{\mu j}), \tag{2}$$

where the coefficients F_{kj} are the corresponding symmetry-dependent weights. In the case of the present CF transitions, the energies of all searched multiplets can be obtained as shown below from the energies of six nonredundant SD's,

$$\begin{aligned}
&E(^4A_{2g}) = E(|\xi^+ \eta^+ \zeta^+|),\\
&E(^4T_{2g}) = E(|\nu^+ \xi^+ \eta^+|),\\
&E(^4T_{1g}(a)) = E(|\mu^+ \xi^+ \eta^+|),\\
&(^4T_{1g}(b)) = E(|\mu^+ \nu^+ \xi^+|),\\
&E(^2E_g) = 1.5^* E(|\xi^+ \nu^+ \zeta^-|) - 0.5^* E(|\xi^+ \eta^+ \zeta^+|),\\
&E(^2T_{1g}) = E(|\xi^- \eta^+ \zeta^-|) + 0.5^* E(|\xi^+ \eta^+ \zeta^+|)\\
&\qquad - 0.5^* E(|\xi^+ \eta^- \zeta^-|),\\
&E(^2T_{2g}) = E(|\xi^- \eta^+ \zeta^-|) - 0.5^* E(|\xi^+ \eta^+ \zeta^+|)\\
&\qquad + 0.5^* E(|\xi^+ \eta^- \zeta^-|),
\end{aligned} \tag{3}$$

where μ and ν are the components of e_g^* ($\sim 3z^2-r^2$ and x^2-y^2, respectively) and ξ, η, and ζ the components of t_{2g}^* ($\sim yz$, xz, and xy, respectively).

In order to obtain the energy of SD's in DFT, we can follow two possible calculation schemes, as described by Daul *et al.*;[35] the so-called transition state (TS) method and the ΔSCF method. As the TS method (for more details, see also Ref. 40) is only well adapted for single interconfigurational excitations, we have chosen the ΔSCF calculation scheme, which is now described with some detail. As is known the KS equations yield an electron density which is totally symmetric in the point group of the system. Thus the ground state of a complex like CrF_6^{3-} can easily calculated using DFT but its application to orbitally degenerated states requires more care and to proceed step by step. Taking as a guide the excited states coming from the $(t_{2g}^*)^2(e_g^*)$ configuration the first step is to solve the KS equations for the average configuration $(\xi^+)^{1/3}(\xi^-)^{1/3}(\eta^+)^{1/3}(\eta^-)^{1/3}(\zeta^+)^{1/3} \times (\zeta^-)^{1/3}(\mu^+)^{1/4}(\mu^-)^{1/4}(\nu^+)^{1/4}(\nu^-)^{1/4}$ whose associated density possess cubic symmetry. In a second step the so obtained KS orbitals are kept frozen and used to calculate the SD's involved in (3) by means of the chosen functional.[33,34,40] For this purpose a very small distortion of the cluster is required so as to obtain for each SD an associated density which is totally symmetric in the point group reached after that symmetry lowering. The present procedure thus takes into account the influence of spin-pairing on the energies of different states emerging from an open shell. Also in a third-step the KS equations can be solved for each SD in a SCF way. As we have verified (Sec. III E) that the energy variations obtained considering the relaxation of the KS orbitals in CF multiplets is practically negligible the results shown here (Table II) have been obtained stopping the calculation at step two.

C. Charge transfer transitions

Rather than calculating the detailed multiplet structure corresponding to each CT one-electron transition, we have performed calculations on the so-called converged unrestricted average of configuration (UAOC) state. This state is a SD that has the right spin and the same number of electrons is placed in each component of a degenerate orbital.

For supporting this view, we can consider the $t_{1u}(\sigma-\pi)\rightarrow e_g^*$ one-electron CT transition. For both $S'=2$ and $S'=1$, there is one resulting multiplet, i.e., $^4T_{2u}$, which has the right symmetry, in order to give rise to dipole allowed CT transitions from the $^4A_{2g}$ ground state. The wave functions of the corresponding UAOC states are then

$$\Psi(^4T_{2u}(S'=2))=|(t_{1u}\uparrow)^2(t_{1u}\downarrow)^3(t_{2g}^*\uparrow)^3(e_g^*\uparrow)^1|,$$
$$\Psi(^4T_{2u}(S'=1))=|(t_{1u}\uparrow)^3(t_{1u}\downarrow)^2(t_{2g}^*\uparrow)^3(e_g^*\downarrow)^1|, \quad (4)$$

where the occupation of the orbitals is as follows: for $^4T_{2u}(S'=2)$ $n_x\uparrow=n_y\uparrow=n_z\uparrow=2/3$, $n_x\downarrow=n_y\downarrow=n_z\downarrow=1$, $n_\xi\uparrow=n_\eta\uparrow=n_\zeta\uparrow=1$, $n_\mu\uparrow=n_\nu\uparrow=1/2$, and for $^4T_{2u}(S'=1)$ $n_x\uparrow=n_y\uparrow=n_z\uparrow=1$, $n_x\downarrow=n_y\downarrow=n_z\downarrow=2/3$, $n_\xi\uparrow=n_\eta\uparrow=n_\zeta\uparrow=1$, $n_\mu\downarrow=n_\nu\downarrow=1/2$. Here *x,y,z* are the components of t_{1u}.

On the other hand, following the method described in Sec. II B, the energy of the $^4T_{2u}$ multiplets can be expressed in function of two SD's,

$$E(^4T_{2u}(S'=2))=2^*E(|x^+y^+x^-y^-z^-\xi^+\eta^+\zeta^+\mu^+|)-E(|x^+y^+z^+x^-y^-\xi^+\eta^+\zeta^+\mu^+|),$$
$$E(^4T_{2u}(S'=1))=2^*E(|x^+y^+z^+x^-y^-\xi^+\eta^+\zeta^+\mu^-|)-E(|x^+y^+x^-y^-z^-\xi^+\eta^+\zeta^+\mu^-|). \quad (5)$$

Then, we have tried the following recipes:

(1) Calculate the SD's following the ΔSCF method, that is, first a restricted run with the excited occupation $(t_{1u})^5(t_{2g}^*)^3(e_g^*)^1$, and then using these orbitals to calculate the SD's of Eqs. (5), using one iteration in a lower symmetry.
(2) Use the same orbitals as in procedure 1 in order to calculate the UAOC's with one iteration in octahedral symmetry.
(3) Construct the UAOC's directly in octahedral symmetry and let the calculation converge.

For an isolated CrF_6^{3-} cluster, using the VWN functional, we have obtained the following results: for $^4T_{2u}(S'=2)$ 6.45 eV, 6.60 eV, and 6.39 eV using recipes 1, 2, and 3, respectively, while for $^4T_{2u}(S'=1)$ 7.57 eV, 7.54 eV, and 7.44 eV were obtained. The small difference between the results from recipes 1 and 2 indicates that we can reasonably use the octahedral approximation in the calculations of CT multiplets. However the difference between recipes 2 and 3 indicates that the involved orbital relaxation is not negligible. For these reasons we have opted for the recipe 3 to calculate CT transition energies.

D. Oscillator strengths

The oscillator strengths corresponding to the nine allowed one-electron CT transitions have been derived by using the TRTSMO 1.1 program[45] that calculates transition dipole moments analytically from a set of KS molecular orbitals obtained with ADF. It has been pointed out that for perturbation calculations the operator involving the dipole moment fulfills the requirements of gauge invariance while it is not the case for the one involving the momentum **p**.[46] For these calculations we have used the KS orbitals corresponding to the $^4A_{2g}$ ground state. In order to check the reliability of the obtained results oscillator strength calculations by using a different procedure have also been carried out. So, we have performed MS-$X\alpha$ calculations on an isolated CrF_6^{3-} cluster, the oscillator strength being obtained through the Noodleman's procedure,[47] which uses the matrix elements of the potential gradient. We have checked that results obtained by using ground state orbitals and the ones corresponding to a Slater's transition state (formed passing half electron from initial to final orbital) are very similar.

III. RESULTS

A. Ground state properties

The equilibrium Cr–F distance, R_e, computed for different clusters using functional within LDA and GGA are collected in Table I. Also the obtained values for the frequency, ω_A and the Grüneisen constant γ_A (Refs. 48, 49) associated with the symmetric A_{1g} mode are reported. The latter constant γ_A is a direct reflect of the anharmonicity of the energy around the equilibrium position making that ω_A also depends on R.[48,49] Similar results to those given in Table I have been found using other functionals.

The computed value for the isolated CrF_6^{3-} unit in the GGA scheme is only about 5% higher than 1.90 Å. The difference is however a little reduced when the effects of the Madelung potential (due to the rest of the K_3CrF_6 lattice) are taken into account. A more important reduction comes however from the inclusion of neighbor ions of the CrF_6^{3-} unit in the $CrF_6K_8K_6^{11+}$ cluster. Although the precise R_e value for the K_3CrF_6 elpasolite is not exactly known,[20] the calculated R_e value for the $CrF_6K_8K_6^{11+}$ appears to be 1.5% smaller than the average Cr–F distance measured for a great deal of compounds.[37] These results suggest that for the calculation of the metal-ligand distance the effect of the next-nearest neighbor exchange and overlap interactions between the complex ion and its surrounding are more important that the one due to purely electrostatic Madelung potential.

The value of $\hbar\omega_A$ computed at the calculated equilibrium distance of an isolated CrF_6^{3-} complex is significantly smaller than the experimental ones lying between 556 cm^{-1} for $Rb_2KGaF_6:Cr^{3+}$ (Ref. 11) and 604 for $K_2NaScF_6:Cr^{3+}$.[12] In the case of a gradient corrected calculation the computed value is about 30% smaller than the experimental one. The inclusion of neighbor ions of CrF_6^{3-} in the calculated cluster improves significantly the agreement with experimental values though the obtained $\hbar\omega_A$ value is now a bit higher than the latter ones.

Also a reduction of the Grüneisen constant γ_A on passing from the CrF_6^{3-} unit alone to the $CrF_6K_8K_6^{11+}$ cluster is obtained as shown in Table I. Although a precise experimental value of the local Grüneisen parameter has not yet been

TABLE I. Calculated values of the equilibrium distance (R_e), angular frequency (ω_A), and Grüneisen constant (γ_A) associated with the symmetric A_{1g} vibration mode corresponding to the electronic ground state $^4A_{2g}$ of Cr^{3+} placed in K_3CrF_6. Aside from the simple CrF_6^{3-} cluster another one involving 21 atoms has been considered in order to explore the influence of further neighbors of Cr^{3+} on the calculated ground state properties. The influence of the Madelung potential due to the *rest of the lattice* is also reported. Results obtained using the local density approximation (VWN functional) or the generalized gradient approximation (BP functional) are both collected. For comparison purpose experimental values of R_e, $\hbar\omega_A$, and γ_A are also given. The figure corresponding to R_e means the average value over a great deal of pure compounds involving CrF_6^{3-} units (Ref. 37) while that associated with $\hbar\omega_A$ is a mean value taken from experimental results for Cr^{3+} doped fluoroelpasolites (Refs. 2–6, 11, 12, 23). The γ_A value has been derived from the Raman spectra of $K_2NaGaF_6:Cr^{3+}$ under pressure (Ref. 12). Values of R_e are given in Å while $\hbar\omega_A$ is given in cm^{-1}.

		R_e		$\hbar\omega_A$		γ_A	
Cluster	Madelung potential	VWN	BP	VWN	BP	VWN	BP
CrF_6^{3-}	Not included	1.957	2.012	438	393	1.85	1.79
CrF_6^{3-}	Included	1.926	1.978	467	423	1.72	1.93
$CrF_6K_8K_6^{11+}$	Not included	1.862	1.882	615	615	1.22	1.14
$CrF_6K_8K_6^{11+}$	Included	1.861	1.880	614	617	0.99	1.08
Experiment		1.90		570		1.8	

reported, the figure computed in the 21 atoms cluster is close indeed to the value $\gamma_A=0.91$ previously calculated in the Hartree–Fock framework.[24] The estimated value of γ_A for $K_2NaGaF_6:Cr^{3+}$ from Raman data under pressure is equal to $\gamma_A=1.8$.[12]

Bearing in mind the results of Table I the significant underestimation of ω_A reached through the calculation on the CrF_6^{3-} unit can now be adscribed to a good extent to the small overestimation of R_e, due to the neglect of close neighbors. In fact, following Grüneisen's law

$$d(\ln\ \omega_A)/d(\ln\ R_e)=-3\,\gamma_A \tag{6}$$

a 5% decrease of the equilibrium distance, R_e, due to pressure would lead to a ~30% increase of ω_A. This simple analysis thus stress the importance of achieving accurate R_e values in the theoretical calculations of impurities in insulators. Otherwise the relative error in R_e will be amplified by the $3\gamma_A$ factor when the frequency of symmetric mode is calculated. In this sense the slight overestimation on the calculated $\hbar\omega_A$ value for the 21 atom cluster can reflect a computed R_e value which is 1.5% smaller than $R_e=1.90$ Å.

It is worth noting that the electronic density on valence orbitals like t_{2g}^* and e_g^* resides practically on the CrF_6^{3-} unit. For instance in the $CrF_6K_8K_6^{11+}$ cluster the electronic density in t_{2g}^* and e_g^* lying outside the CrF_6^{3-} complex has been found to be smaller than 1%. From this result one can thus expect that optical transition energies can reasonably be accounted for considering *only* the single CrF_6^{3-} unit. As it has already been pointed out the equilibrium distance of the CrF_6^{3-} complex cannot however be completely understood ignoring the closer ions in the host lattice. This result is thus in agreement with previous findings on $3d$ impurities at cubic sites on insulators where the Madelung potential due to the rest of the lattice is nearly flat.[21,33,50,51]

Although the electronic properties due to a $3d$ cation in a cubic site of an insulator can thus be explained essentially on the basis of the complex formed by the $3d$ ion and the ligands this is not in principle true for a vibrational parameter like ω_A. In fact, when in the present case the F^- ligands move from their equilibrium positions there is also a change of the distance to the nearest fixed K^+ ions which should also contribute to the total force constant k_T. In a simple model $k_T=k_c+k_r$ where k_c comes from the CrF_6^{3-} complex and k_r reflects the interaction between this complex and the first K^+ neighbors. The present analysis allows one to estimate the ratio k_c/k_T for the studied system. So, by means of data gathered in Table I and Eq. (6) is possible to evaluate $\hbar\omega_A$ corresponding to CrF_6^{3-} but at the equilibrium distance of the $CrF_6K_8K_6^{11+}$ cluster. Taking the data for the BP functional, we have that $\hbar\omega_A$ for CrF_6^{3-} at 1.88 Å would be equal to 540 cm^{-1}. That figure is thus only 12% smaller than the value $\hbar\omega_A=615$ cm^{-1} computed for cluster where the interaction between F^- and the fixed nearest K^+ ions in the A_{1g} mode is included. This result thus indicates that $k_c/k_T\approx 75\%$.

Bearing in mind this result one should expect that changes of ω_A induced by changing the host lattice would mainly reflect the variations undergone by R. From the analysis of experimental 10 Dq data it is concluded (Sec. III B) that R in $K_2NaAlF_6:Cr^{3+}$ is about 2.5 pm smaller than in $Rb_2KGaF_6:Cr^{3+}$.[11] As regards $\hbar\omega_A$ it increases on passing from the latter ($\hbar\omega_A=556$ cm^{-1}) to the former system ($\hbar\omega_A=575$ cm^{-1}) indeed. Moreover, if the k_r contribution is disregarded in the analysis, these experimental data suggest a value of γ_A close to 2.

B. Crystal field excited states

The calculated values of CF transitions observed in optical absorption spectra of K_3CrF_6 are collected in Table II. Such transitions have been calculated at the equilibrium Cr^{3+}–F^- distance of the ground state that, as discussed in the previous section, is dependent on the cluster size. As representative data only the results obtained for isolated CrF_6^{3-} and $CrF_6K_8K_6^{11+}$ clusters using the GGA functional are reported in Table II. When looking upon the first excited state $^4T_{2g}$, which is responsible for the luminescence at ambient pressure, it is seen that the $^4A_{2g}\rightarrow{}^4T_{2g}$ absorption tran-

TABLE II. Calculated optical absorption transition energies (given in cm^{-1}) for K_3CrF_6 using two different clusters and the functional by Becke and Perdew (Refs. 34, 35). Transition energies have been computed at the *calculated* equilibrium metal-ligand distance which is equal to $R_e=2.012$ Å for CrF_6^{3-} and $R_e=1.882$ Å for $CrF_6K_8K_6^{11+}$. The value of the exponent n [defined in (7)] expressing the *sensitivity* of 10 Dq to R changes is also given. The experimental crystal-field transitions associated with K_3CrF_6 (Ref. 20) are included for comparison.

Transition energies	CrF_6^{3-}	$CrF_6K_8K_6^{11+}$	Experiment
$^4A_{2g}\rightarrow{}^4T_{2g}$	12743	18626	15200
$^4A_{2g}\rightarrow{}^4T_{1g}$ (a)	21374	27530	21800
$^4A_{2g}\rightarrow{}^4T_{1g}$ (b)	28041	39737	35000
$^4A_{2g}\rightarrow{}^2E_g$	11045	10810	16300
$^4A_{2g}\rightarrow{}^2T_{1g}$	15682	15444	16300
$^4A_{2g}\rightarrow{}^2T_{2g}$	23045	22651	23000
n	3.98	4.07	

sition energy is slightly underestimated in the 7 atom cluster, while it increases significantly on passing to the 21 atom cluster. This effect can partially be ascribed to the different equilibrium distance reached for both clusters.

In the ligand-field scheme the $^4A_{2g}\rightarrow{}^4T_{2g}$ transition energy is just equal to 10 Dq, a parameter which has been shown to be strongly dependent upon R.[52,53] The microscopic origin of this important property has recently been clarified.[54] Writing

$$10\ \mathrm{Dq}=KR^{-n}, \tag{7}$$

the calculated values of the exponent n are also given in Table II, being close to four for the present case. From experimental data on Cr^{3+} doped fluoro-elpasolites a value $n=4.5$ has been estimated.[12] Therefore a decrement of 0.13 Å in the equilibrium distance of the CrF_6^{3-} complex alone would lead to an increase of the $^4A_{2g}\rightarrow{}^4T_{2g}$ transition energy close to 5500 cm^{-1}.

The law (7) is useful for measuring the R variation induced by a change in the host lattice. For instance, the zero phonon line related to the $^4A_{2g}\rightarrow{}^4T_{2g}$ transition appears at 14 383 cm^{-1} for $Rb_2KGaF_6:Cr^{3+}$ but at 15 142 cm^{-1} for $K_2NaAlF_6:Cr^{3+}$.[11] According to (7) that variation indicates that the difference, ΔR, between the corresponding Cr^{3+}–F^- distances is only of 2.5 pm.

A similar situation to that found for $^4A_{2g}\rightarrow{}^4T_{2g}$ transition also occurs for other transitions involving the $(t_{2g}^*)^2(e_g^*)^1$ configuration which are thus dependent on 10 Dq. The $^4T_{1g}(b)$ state is better reproduced that the $^4T_{1g}(a)$ one using the $CrF_6K_8K_6^{11+}$ cluster.

The transition energy to the excited states mainly built from the $(t_{2g}^*)^3$ configuration is calculated to have practically the same value in both type of clusters. This effect reflects the very small R dependence displayed by Racah parameters. Although the pressure dependence of Racah parameters B and C has not been reported for Cr^{3+} in fluorides, experimental results have been obtained for ruby.[53] Writing

$$B=B_0R^{-n_B},\qquad C=C_0R^{-n_C}, \tag{8}$$

values of $n_B=1.5$ and $n_C=-0.2$ have been obtained for the latter case.[53] This fact would be related to the nearly independence on R displayed by the transferred spin density on the $2p\sigma$ ligand orbitals which has recently been discussed.[54]

Considering the overall CF transition energies given in Table II, the agreement between experimental and calculated values is rather good, with an average relative error ~20%. Despite this fact the most significant discrepancy between the calculated and experimental CF absorption spectrum concerns the nature of the first excited state. In fact, for Cr^{3+} in fluorides at ambient pressure[5,13,20] the two $^4A_{2g}\rightarrow{}^4T_{2g}$ and $^4A_{2g}\rightarrow{}^2E_g$ transitions are practically coincident and so the emission comes from the relaxed $^4T_{2g}$ state as the electron–phonon coupling in the 10 Dq-independent ^2E_g state is negligible. A similar situation to this one was recently encountered in the calculations on Cr^{3+} doped chloro-elpasolites carried out using $CrCl_6^{3-}$ 7 atom clusters.[33] In that case the separation between ^2E_g and $^4T_{2g}$ states obtained through the GGA functional is only 2000 cm^{-1} similarly to what is found in the present calculation on the isolated CrF_6^{3-} complex (Table II). We have verified that on passing from $CrCl_6^{3-}$ to a 21 atom cluster R_e is again reduced, the reduction being ~3%.

C. Coupling with vibrations for the $^4T_{2g}$ state: Stokes shift

Let us now focus on the coupling between the $^4T_{2g}$ state and the vibrations of the CrF_6^{3-} unit, which determines a parameter as important as the Stokes shift. The experimental emission spectra at low temperatures reported for Cr^{3+} in fluorides reveals progressions involving the two even stretching A_{1g} and E_g modes.[2,4,6,11] As it is well known, the coupling with the Jahn-Teller mode, E_g, for an excited T_{2g} state does not lead to a splitting of the absorption band but only to the appearance of the corresponding progressions in the low temperature spectra.[55] Therefore, for that case the influence of the Jahn-Teller mode on the optical spectrum is identical to that coming from the coupling with the symmetric A_{1g} mode and so the experimental Stokes shift measured at room temperature, can simply be written for the present case as

$$E_s=E_s(A)+E_S(E). \tag{9}$$

Here, $E_S(i)$ $(i=A,E)$ means the partial contribution to the Stokes shift due to one mode alone which can be expressed as follows:[26]

$$E_S(i)=2S_i\hbar\omega_i,\qquad S_i=V_i^2/(2M_L\hbar\omega_i^3), \tag{10}$$

where S_i $(i=A,E)$ is the Huang–Rhys factor, V_i the coupling constant, and M_L is the ligand mass.[26] These expressions are valid assuming linear coupling and thus implies that the frequency of vibration modes is the same for both the ground and the excited state. For the present case ω_A in $^4T_{2g}$ is calculated to differ by 1% from that computed for the ground state in the 21 atom cluster.

The results on Huang–Rhys factors and Stokes shift reached through the present calculations are displayed in Table III. As the experimental E_S values for Cr^{3+} in fluo-

TABLE III. Calculated values of the Huang–Rhys factors (S_A and S_E), the partial Stokes shifts ($E_S(A)$ and $E_S(E)$) and the total Stokes shift (E_S) reflecting the coupling with the symmetric A_{1g} and the Jahn-Teller E_g mode. The results obtained on an isolated CrF_6^{3-} and on a $CrF_6K_8K_6^{11+}$ cluster using the functional by Becke and Perdew (Refs. 34, 35) are both shown. For both clusters all the parameters have been computed at the *calculated* equilibrium metal-ligand distance. For comparison the range of experimental $\hbar\omega_A$, $\hbar\omega_E$ (Refs. 2–6, 11, 12, 23) and E_S (Refs. 14, 23) values measured for Cr^{3+} doped fluoroelpasolites is also given. Estimated values (Refs. 26, 52) of S_A, S_E, $E_S(A)$, and $E_S(E)$ are reported as well. The values of $\hbar\omega_A$, $E_S(A)$, $\hbar\omega_E$, $E_S(E)$, and E_S are all given in cm^{-1} units.

	CrF_6^{3-}	$CrF_6K_8K_6^{11+}$	Experiment
S_A	1.54	0.94	0.6–1.1
$\hbar\omega_A$	393	615	556–604
$E_S(A)$	1207	1158	~1100
S_E	2.4	0.72	1–1.5
$\hbar\omega_E$	266	542	465–510
$E_S(E)$	1284	782	~1300
E_S	2591	1940	2300–2700

TABLE IV. Calculated values of the energy (in eV) corresponding to the allowed charge transfer transitions for the CrF_6^{3-} chromophore in K_3CrF_6. The results obtained at the *calculated* equilibrium metal-ligand distance on an isolated CrF_6^{3-} and on a $CrF_6K_8K_6^{11+}$ cluster using the functional by Becke and Perdew (Refs. 34, 35) are both shown. The transition energies corresponding to an isolated complex but calculated at $R=1.88$ Å are also displayed.

	CrF_6^{3-} ($R=2.01$ Å)	CrF_6^{3-} ($R=1.88$ Å)	$CrF_6K_8K_6^{11+}$
$t_{1u}(\sigma-\pi)\uparrow\rightarrow e_g^*\uparrow$	5.93	7.05	7.91
$t_{1u}(\sigma-\pi)\downarrow\rightarrow t_{2g}^*\downarrow$	6.94	8.18	7.83
$t_{1u}(\sigma-\pi)\downarrow\rightarrow e_g^*\downarrow$	6.99	8.18	9.33
$t_{1u}(\sigma+\pi)\uparrow\rightarrow e_g^*\uparrow$	6.75	8.00	8.94
$t_{1u}(\sigma+\pi)\downarrow\rightarrow t_{2g}^*\downarrow$	7.72	9.05	8.81
$t_{1u}(\sigma+\pi)\downarrow\rightarrow e_g^*\downarrow$	7.81	9.05	10.31
$t_{2u}\uparrow\rightarrow e_g^*\uparrow$	5.87	7.00	8.06
$t_{2u}\downarrow\rightarrow t_{2g}^*\downarrow$	6.86	8.11	8.14
$t_{2u}\downarrow\rightarrow e_g^*\downarrow$	6.91	7.48	9.32

rides are found to be in the 2300–2700 cm^{-1} range[14] the calculated ones in Table III are not far from it. Though E_S calculated for CrF_6^{3-} is in better agreement with experimental values than using the 21 atom cluster, the S_A, S_E values as well as the frequencies are however much better reproduced in the latter case. In this sense S_E has been estimated to be equal to 1.2 for $Rb_2KGaF_6:Cr^{3+}$ while S_A would be in the 0.6–1.1 range.[26,56]

Although the calculated value of $E_S(A)$ for both clusters is practically the same, this has to be regarded as a coincidence. In fact, $E_S(A)$ depends[22] on the ratio V_A^2/ω_A^2, where both quantities strongly depend on the metal-ligand distance R. As it has been pointed out[22,26] in the present case V_A depends on $d(10\,Dq)/dR$ and thus V_A is proportional to $R^{-(n+1)}$. Therefore, the significant increase experienced by ω_A on passing from CrF_6^{3-} to $CrF_6K_8K_6^{11+}$ is compensated by the corresponding one due to V_A.

In comparison with the experimental values of ω_E (lying in the 465–510 cm^{-1} range)[4,11,12,23] the present calculations for the 21 atom cluster lead to an average overestimation of 13% for ω_E which is higher than that obtained for the symmetric A_{1g} mode. This overestimation is partially responsible for the underestimation of S_E in comparison with experimental values. It is worth noting however that if we take $\hbar\omega_E=480\ cm^{-1}$ from experiments[2,11] instead of $\hbar\omega_E=542\ cm^{-1}$ found in the calculation for $CrF_6K_8K_6^{11+}$ then Eq. (10) would lead to $S_E=1.05$ and $E_S(E)=1000\ cm^{-1}$.

The present values calculated for the 21 atom cluster can also be compared to preceding ones obtained in the Hartree–Fock scheme. For instance, Woods *et al.*[23] obtain $E_S(E)=782\ cm^{-1}$ and $E_S(A)=990\ cm^{-1}$, which are close to those obtained in the present calculations for a 21 atom cluster. In the calculations by Seijo *et al.*[24] $E_S(A)$ is found to be equal only to 600 cm^{-1}.

D. Allowed charge-transfer transitions: Energy and oscillator strength

The calculated values corresponding to the allowed CT transitions of the CrF_6^{3-} cromophore are reported in Table IV. Aside from the results obtained for CrF_6^{3-} and $CrF_6K_8K_6^{11+}$ at the equilibrium metal-ligand distances $R_e=2.01$ Å and $R_e=1.88$ Å, respectively, the calculated values at $R=1.88$ Å for the former cluster are also included. The comparison between the energies calculated for CrF_6^{3-} at two different distances underlines the significant dependence of CT energies on R.[27] As previously discussed for Cr^{3+} and other impurities[27] a decrement of R induces a blue shift of CT transitions. The results collected in Table IV do support the existence of allowed CT transitions due to the CrF_6^{3-} chromophore in the 7–14 eV range. A similar conclusion was recently reached[27] from MS-$X\alpha$ and SCCEH calculations on CrF_6^{3-} carried out at $R=1.90$ Å.

For gaining a better insight into the experimental spectrum of Fig. 1, the oscillator strength associated with each one of the allowed transitions has been calculated. Apart from the results obtained for restricted ADF calculations those reached using the unrestricted MS-$X\alpha$ method for CrF_6^{3-} are also reported in Table V. As main trend such results indicate that the highest oscillator strengths are found for transitions involving $t_{1u}(j)$ ($j=\sigma+\pi;\sigma-\pi$) and e_g^* orbitals. In particular the highest oscillator strength appear for the $t_{1u}(\sigma+\pi)$ orbital. Comparing $t_{1u}(j)\uparrow\rightarrow e_g^*\uparrow$ with $t_{1u}(j)\downarrow\rightarrow t_{2g}^*\downarrow$ transitions the oscillator strength of the former is in general much higher than that of the later. Therefore combining the data given in Tables IV and V, it is reasonable to assign peaks A (at $E=8.0$ eV) and B (at $E=8.7$ eV) as arising mainly from $t_{1u}(\sigma-\pi)\uparrow\rightarrow e_g^*\uparrow$ and $t_{1u}(\sigma+\pi)\uparrow\rightarrow e_g^*\uparrow$ transitions, respectively. This assignment is thus in agreement with the previous one.[27]

Some problems are found in the present calculations with respect to $e_g^*\downarrow$ orbitals. In particular the spin-polarization splitting between $e_g^*\uparrow$ and $e_g^*\downarrow$ orbitals is found to be ~1 eV smaller than that predicted by the empirical rule by Adachi *et al.*[57] On the other hand in the 21 atom cluster the $e_g^*\downarrow$ orbital is found to lie just below the levels coming from the $4s$ levels of involved K atoms. In view of these arguments and the results of Tables IV and V it is still reasonable to assign the C peak in Fig. 1 which appears at $E=12.0$ eV to the $t_{1u}(\sigma+\pi)\downarrow\rightarrow e_g^*\downarrow$ transition.

TABLE V. Calculated values of the oscillator strength corresponding to the *allowed* charge transfer transitions for the CrF_6^{3-} chromophore in K_3CrF_6. The results obtained through spin restricted calculations at the *calculated* equilibrium metal–ligand distance on CrF_6^{3-} ($R_e=2.01$ Å) and $CrF_6K_8K_6^{11+}$ ($R_e=1.88$ Å) clusters using the functional by Becke and Perdew (Refs. 34, 35) are both shown. The results obtained on the CrF_6^{3-} cluster through spin unrestricted MS-$X\alpha$ calculations at $R=1.91$ Å are also displayed for comparison.

	CrF_6^{3-} (MS-$X\alpha$)	CrF_6^{3-}	$CrF_6K_8K_6^{11+}$
$t_{1u}(\sigma-\pi)\uparrow\rightarrow e_g^*\uparrow$	0.112	0.073	0.104
$t_{1u}(\sigma-\pi)\downarrow\rightarrow t_{2g}^*\downarrow$	0.035	0.049	0.047
$t_{1u}(\sigma-\pi)\downarrow\rightarrow e_g^*\downarrow$	0.106	0.073	0.104
$t_{1u}(\sigma+\pi)\uparrow\rightarrow e_g^*\uparrow$	0.093	0.150	0.125
$t_{1u}(\sigma+\pi)\downarrow\rightarrow t_{2g}^*\downarrow$	0.010	0.008	0.017
$t_{1u}(\sigma+\pi)\downarrow\rightarrow e_g^*\downarrow$	0.050	0.150	0.125
$t_{2u}\uparrow\rightarrow e_g^*\uparrow$	0.000	0.001	0.000
$t_{2u}\downarrow\rightarrow t_{2g}^*\downarrow$	0.060	0.065	0.073
$t_{2u}\downarrow\rightarrow e_g^*\downarrow$	0.010	0.001	0.000

Comparing the oscillator strength of the nine transitions analyzed in Table V it appears that the transitions $t_{2u}(h)\rightarrow e_g^*(h)$ $(h=\uparrow;\downarrow)$ exhibit an oscillator strength which is much smaller than that due to the rest of transitions. This important fact can be explained to some extent taking into account the form of all orbitals involved in Table V. An orbital $|\gamma\rangle$ of CrF_6^{3-} belonging to the γ representation can be written in a simple molecular orbital description as follows:

$$|\gamma\rangle=\alpha|d;\gamma\rangle-\beta|\chi_L;\gamma\rangle,$$
$$|\chi_L;\gamma\rangle=\sum C_{k,i}|p_i^k\rangle, \tag{11}$$

where $k=1,...,6$ denotes the six involving ligands while the index $i=x,y,z$ refers to the three possible components of an atomic $2p$ orbital.

Let us consider an allowed CT transition, depicted as $\gamma\rightarrow\gamma'$. If the same $|p_i^k\rangle$ orbital appears in both $|\gamma\rangle$ and $|\gamma'\rangle$ wave functions, then the associated dipole matrix element contains a term like $\langle p_i^k|\mathbf{r}|p_i^k\rangle$. This term is practically equal to $\mathbf{R}_k$ (corresponding to the position vector of the *k*-ligand) and thus reflects the size of the octahedral complex. Aside from this first class of allowed CT transitions, in the second one another $|p_j^k\rangle$ orbital $(j\neq i)$ is involved in $|\gamma'\rangle$ leading to dipole matrix elements reflecting the radius of the ligand ion rather than the molecule size. Following this semiquantitative argument in octahedral complexes transitions where both $|\gamma\rangle$ and $|\gamma'\rangle$ orbitals exhibit either the σ or π-character belong to the first class. By contrast, when $|\gamma\rangle$ has a σ-character while $|\gamma'\rangle$ has a π-character, or vice versa, the transition belongs to the second class. As t_{2u} is a π-orbital while e_g^* has a σ-character transitions involving both orbitals clearly belong to the second class. Because of the strong (π,σ) mixing in the $t_{1u}(\sigma-\pi)$ and $t_{1u}(\sigma+\pi)$ orbitals the rest of the transitions analyzed in Table V belong to the first class.

It can be expected that a transition of the type $t_{1u}\rightarrow e_g^*$ will increase its oscillator strength as far as the σ-character of the t_{1u} orbital increases. By the same reason the oscillator strength of a $t_{1u}\rightarrow t_{2g}^*$ transition will be increased by decreasing the σ-character in t_{1u}. This idea is in general followed by the results contained in Table V. For instance, considering first the CrF_6^{3-} unit, in the orbital called $t_{1u}(\sigma-\pi)$ the σ-character is found to be 25% while in $t_{1u}(\sigma+\pi)$ that character amounts to 75%. In this case the oscillator strength calculated for the $t_{1u}(\sigma+\pi)\uparrow\rightarrow e_g^*\uparrow$ transition is practically twice that of the $t_{1u}(\sigma-\pi)\uparrow\rightarrow e_g^*\uparrow$. This ratio is however reduced to 1.2 in the $CrF_6K_8K_6^{11+}$ cluster, where the σ-character for $t_{1u}(\sigma-\pi)$ and $t_{1u}(\sigma+\pi)$ is 40% and 60%, respectively.

The present ideas are also useful for explaining the main trends displayed by the intensities due to CT transitions of other complexes. For instance, in the D_{4h} $CuCl_6^{4-}$ chromophore[30] the unpaired electron lies in the $b_{1g}(\sim x^2-y^2)$ σ-orbital and the experimental CT spectrum is essentially due to jumps from $e_u(\sigma-\pi)$ and $e_u(\sigma+\pi)$ orbitals as no experimental evidence from the allowed transition involving the b_{2u} π-orbital has been reported. On the contrary, in the octahedral MoF_6 molecule[58] the lowest CT transitions involve jumps to the t_{2g}^* antibonding π-orbital which is empty in the ground state. In this case the oscillator strength of CT transitions involving t_{1u} orbitals increase significantly with the content of the π-character.[58]

The local lattice relaxation in an excited CT state deserves also some comments. In Fig. 2 the potential energy curve calculated as a function of the Cr–F distance for the $^4T_{2u}(S'=2)$ CT state associated with the $t_{1u}(\sigma-\pi)\uparrow\rightarrow e_g^*\uparrow$ jump is depicted. For comparison the plots corresponding to the $^4T_{2g}$ and $^4T_{1g}$ CF states as well as the ground state $^4A_{2g}$ are also included. In the three excited states the equilibrium distance, R_e^*, is higher than R_e corresponding to the ground state. Nevertheless in the CF states R_e^* differs from R_e by 1.5%, while this difference is 3.4 times bigger in the case of the CT $^4T_{2u}$ state. The value $R_e^*=1.981$ Å found for this CT state leads to a Huang–Rhys factor $S_A=11$, which is thus an order of magnitude higher than that corresponding to the $^4T_{2g}$ CF state.

This important difference between CT and CF states reflects the different origin of the coupling constant V_A. For instance, V_A for the considered $^4T_{2u}$ CT state reflects the *R* sensitivity of the $e_g^*\uparrow$ energy, which in turn mainly reflects the variation of the electrostatic potential on *d*-electrons due to close anions.[27] By contrast, V_A for the $^4T_{2g}$ CF state mainly comes from the variations of the splitting 10 Dq to *R* changes.[22,54] In the present case V_A is found to be equal to 150 meV/pm for $^4T_{2u}$, while $V_A=50$ meV/pm for $^4T_{2g}$.

The value $S_A=11$ reached for the CT $^4T_{2u}(S'=2)$ state implies a bandwidth $W=0.6$ eV, considering only the coupling to the A_{1g} mode. This value is close to $W=0.7$ eV estimated for bands *A* and *B* from the experimental spectrum at $T=10$ K.[9] Similar results to these ones were derived recently through MS-$X\alpha$ and SCCEH methods.[27]

As regards the ω_A frequency in the $^4T_{2u}(S'=2)$ CT state the present calculations indicate that it is ~4% smaller than in the ground state. The validity of this result cannot however be checked, as no progressions are seen in the low temperature excitation spectrum. This fact can be related to

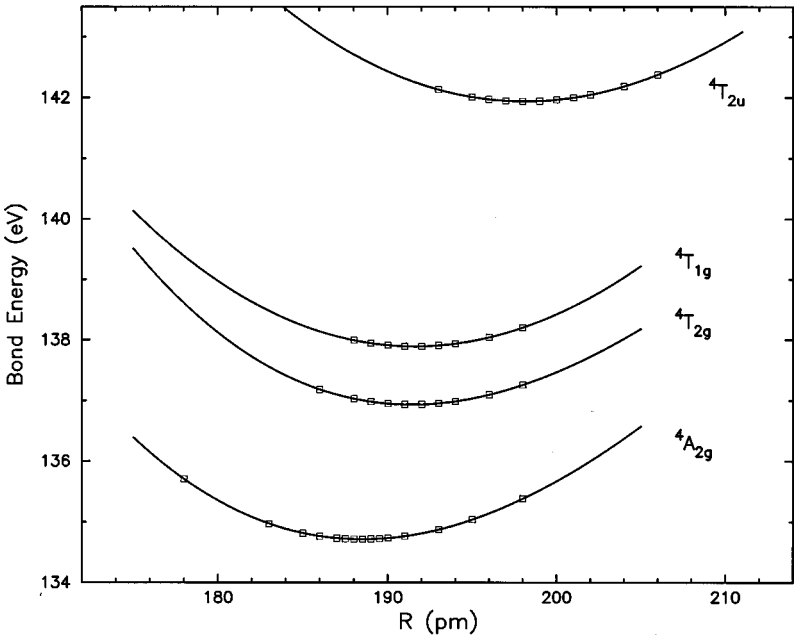

FIG. 2. Energy of the ground state ($^4A_{2g}$) and several excited states obtained for the $CrF_6K_8K_6^{11+}$ cluster as a function of the metal–ligand distance, *R*. All the calculations have been carried out using the generalized gradient approximation (BP functional). Results are shown for the $^4T_{2g}$ and $^4T_{1g}$ states involved in the spin allowed crystal-field transitions as well as for the $^4T_{2u}$ state formed through a $t_{1u}(\sigma-\pi)\uparrow \rightarrow e_g^*\uparrow$ charge transfer excitation. The calculated equilibrium distance for both crystal field states is only 1.5% higher than that for the ground state. For the charge transfer state such a difference amounts however to 5.1% thus implying a much bigger ligand relaxation.

the strong coupling with A_{1g} mode in CT states, a fact that does not favor the experimental observation of the individual components of a vibrational progression.

E. Electronic relaxation in excited states

When a complex like CrF_6^{3-} goes from the ground to an excited state by absorption of a photon, not only the one-electron KS orbitals population changes, but also the involved wave functions. This electronic relaxation leads to modifications of the transition energy and the charge on different atoms. The results for a $t_{1u}(\sigma-\pi)\rightarrow e_g^*$ CT transition in CrF_6^{3-} are shown in Table VI.

When the properties of the $^4T_{2u}(S'=2)$ excited state are calculated keeping the same KS orbitals of the ground state, the total charge on chromium decreases by 0.76 *e* with respect to the $^4A_{2g}$ state. At this stage, an important transfer of charge from ligands to the central ion has thus taken place. When electronic relaxation is allowed to occur the variation is, however, reduced to -0.20 *e* in accord with previous results on $d^n(n=0,1,2)$ tetraoxo complexes.[38–40] This important flow of charge to the ligands containing a hole, which appears in the relaxation process, also leads to a significant diminution ($\sim$40%) of the CT energy. The direction of this effect is reasonable as an increase of the total charge on chromium decreases the energy of mainly $3d$ levels and thus the energy of CT transitions.

TABLE VI. Electronic relaxation effects associated with the $^4T_{2u}$ state created in the allowed $t_{1u}(\sigma-\pi)\uparrow \rightarrow e_g^*\uparrow$ transition. *E* (in eV) means the energy of such a transition and ΔQ represents the variation of the total charge on chromium taking as reference that of the $^4A_{1g}$ ground state. In the unrelaxed calculation the Kohn–Sham orbitals for the excited state are the same as those for $^4A_{1g}$ while in the relaxed calculation the full SCF procedure in the excited state has taken place.

Calculation	ΔQ	*E*
Unrelaxed	$-0.76e$	12.1
Relaxed	$-0.20e$	7.9

Aside from stressing the key role played by the electronic relaxation for a good understanding of CT transitions, the present results and those previously reached on d^0 systems[38–40] indicate that some simple models previously used can be improved. For instance, in the case of nearly ionic complexes due to M^{n+} cations embedded in the same lattice, it has been proposed[59] that the CT transition energy, E_{CT}, can be written approximately as

$$E_{CT}=C-I_{n-1}, \tag{12}$$

where *C* depends on the host lattice and I_{n-1} is the $n-1$ ionization potential of M. The present analysis suggest that I_n, rather than I_{n-1}, should be used for ionic complexes.

As expected, the electronic relaxation calculated for an excited CF state is much smaller than that obtained for CT states. For instance, for the $^4T_{2g}$ CF state the electronic relaxation induces an energy decrement that is calculated to be equal only to 0.2 eV.

IV. FINAL REMARKS

A good number of geometrical, vibrational and optical parameters associated with sixfold coordinated Cr^{3+} impurities in fluorides have been investigated by means of ADF calculations carried out on CrF_6^{3-} and $CrF_6K_8K_6^{11+}$ clusters. From the present study a reasonable agreement between the calculated vibrational frequencies, 10 Dq-dependent CF transitions, Huang–Rhys factors or CT transition energies and the corresponding experimental values, is achieved only if the calculated equilibrium metal-ligand distance is very close to the experimental one. In fact, as already stressed a 6% error in R_e can lead for instance to a 40% error in the computed frequencies or to a 25% error in 10 Dq. Although the equilibrium distance reached for a 21 atom cluster is essen-

tially coincident with the average R_e value measured for Cr^{3+} in fluorides, it is also true that optical properties due to Cr^{3+} ions can be well explained considering only the CrF_6^{3-} unit alone but at the right equilibrium distance. In the same vein optical transitions and coupling constants due to Cr^{4+} in oxides are reasonably explained through ADF calculations of the simple CrO_4^{4-} unit carried out around 1.7 Å.[60]

Aside from providing reasonable results about the Stokes shift and the electron-vibration coupling in the $^4T_{2g}$ CF state, the CT transitions due to CrF_6^{3-} in fluorides have also been explored through the present work. The analysis carried out on oscillator strengths allows one to understand what are, among the nine allowed transitions, the less intense ones and what is the main reason for it. The idea that $\gamma \rightarrow \gamma'$ jumps where both exhibit the same σ- or π-character lead to a higher oscillator strength that in the opposite cases, also explains the CT spectra of $CuCl_6^{4-}$, $NiCl_6^{4-}$ or MoF_6.[58,59]

Though the overall description of CF multiplets using the procedure explained in Sec. II A is rather good, it fails however to predict correctly the position of the 10 Dq-independent ^2E_g state with respect to $^4T_{2g}$. Another problem found through this work concerns the nature of excited one-electron levels like $e_g^*\downarrow$ whose description could be improved using bigger clusters.

CF transitions due to the CrF_6^{3-} complex alone have been calculated using the Hartree–Fock (HF) method and subsequent configuration interaction involving the diagonalization of matrices of size up to 555 000.[20] In this case R_e was fixed to be equal to 1.93 Å and the maximum deviation between experimental and theoretical transition energies was found to be 3000 cm^{-1}. Though this discrepancy is a bit smaller than that obtained in this work the present DFT calculations also provides a reasonable understanding of CT transitions which up to now has not been achieved using the HF methodology. It has recently been pointed out[61] that a lack of convergence is found when the CT transitions of tetraoxo complexes (involving Cr^{4+}, Mn^{5+} or Fe^{6+} ions) are tried to be calculated using the multiconfiguration complete active space SCF (CASSCF) method.

Therefore DFT methods offer advantages for exploring a great deal of properties due to an impurity, M, when their active electrons are not localized within the region corresponding to the MX_N complex formed by M and the N closest anions. This situation occurs not only in semiconductor lattices but also for neutral atoms (like Ag^0) placed in a lattice like KCl, where the unpaired electron is close to the bottom of the conduction band.[62] In this case calculations where more than 50 atoms are treated on the same footing become necessary.

Finally the present results and those in Ref. 33 indicate that DFT methods also lead to a reasonable description of excited states of transition metal complexes using the same functional employed for calculating ground state properties.

ACKNOWLEDGMENT

This work has been partially supported by the CICYT under Project No. PB95-0581.

[1] C. K. Jørgensen, *Absorption Spectra and Chemical Bonding in Complexes* (Pergamon, London, 1962).
[2] J. Ferguson, H. J. Guggenhein, and D. L. Wood, J. Chem. Phys. **54**, 504 (1971).
[3] L. Dubicki, J. Ferguson, and B. Van Oosterhout, J. Phys. C **13**, 2791 (1980).
[4] P. Greenough and A. G. Paulusz, J. Chem. Phys. **70**, 1967 (1979).
[5] J. F. Dolan, L. A. Kappers, and R. H. Bartram, Phys. Rev. B **33**, 7339 (1986).
[6] S. A. Payne, L. L. Chase, and G. D. Wilke, J. Lumin. **44**, 167 (1989).
[7] H. W. H. Lee, Stephen, A. Payne, and L. L. Chase, Phys. Rev. B **39**, 8907 (1989).
[8] R. Wannemacher and R. S. Meltzer, J. Lumin. **43**, 251 (1989).
[9] D. de Viry, M. Casalboni, M. Palummo, and N. Zema, Solid State Commun. **76**, 1051 (1990).
[10] T. P. J. Han, F. Jaque, C. Trager-Cowan, K. P. O'Donnell, and B. Henderson, Appl. Phys. A: Solids Surf. **53**, 209 (1991).
[11] C. Marco de Lucas, F. Rodriguez, J. M. Dance, M. Moreno, and A. Tressaud, J. Lumin. **48&49**, 553 (1991).
[12] J. F. Dolan, A. G. Rinzler, L. A. Kappers, and R. H. Bartram, J. Phys. Chem. Solids **53**, 905 (1992).
[13] P. T. C. Freire, O. Pilla, and V. Lemos, Phys. Rev. B **49**, 9232 (1994).
[14] M. C. Marco de Lucas, J. M. Dance, F. Rodríguez, A. Tressaud, M. Moreno, and J. Grannec, Radiat. Eff. Defects Solids **135**, 19 (1995).
[15] M. Mortier, Q. Wang, J. Y. Buzaré, M. Rousseau, and B. Piriou, Phys. Rev. B **56**, 3022 (1997).
[16] S. A. Payne, L. L. Chase, L. K. Smith, W. L. Kway, and H. W. Newkirk, J. Appl. Phys. **66**, 1051 (1989).
[17] Z. Zhang, K. T. V. Grattan, and A. W. Palmer, Phys. Rev. B **48**, 7772 (1993).
[18] L. Pueyo and J. W. Richardson, J. Chem. Phys. **67**, 3577 (1977); **67**, 3583 (1977).
[19] Z. Barandiaran and L. Pueyo, J. Chem. Phys. **79**, 1926 (1983).
[20] K. Pierloot and L. G. Vanquickenborne, J. Chem. Phys. **93**, 4154 (1990).
[21] K. Pierloot, E. Van Praet, and L. G. Vanquickenborne, J. Chem. Phys. **96**, 4163 (1992).
[22] M. Moreno, M. T. Barriuso, and J. A. Aramburu, J. Phys.: Condens. Matter **4**, 9481 (1992).
[23] A. M. Woods, R. S. Sinkovits, J. Charpie, W. L. Huang, R. H. Bartam, and A. R. Rossi, J. Phys. Chem. Solids **54**, 543 (1993).
[24] L. Seijo, Z. Barandiaran, and L. G. M. Petterson, J. Chem. Phys. **98**, 4041 (1993).
[25] A. M. Woods, R. S. Sinkovits, and R. H. Bartram, J. Phys. Chem. Solids **55**, 91 (1994).
[26] M. T. Barriuso, J. A. Aramburu, and M. Moreno, Phys. Status Solidi B **193**, 193 (1996).
[27] J. A. Aramburu, M. T. Barriuso, and M. Moreno, J. Phys.: Condens. Matter **8**, 6901 (1996).
[28] D. M. Calistru, S. G. Demos, and R. R. Alfano, Phys. Rev. B **52**, 15253 (1995).
[29] M. Couzi, M. Moreno, and A. G. Breñosa, Solid State Commun. **91**, 481 (1994).
[30] M. T. Barriuso, J. A. Aramburu, C. Daul, and M. Moreno, Int. J. Quantum Chem. **61**, 563 (1997), and references therein.
[31] E. J. Baerends, D. E. Ellis, and P. Ros, Chem. Phys. **2**, 41 (1973).
[32] B. te Velde and E. J. Baerends, J. Comput. Phys. **99**, 84 (1992).
[33] F. Gilardoni, J. Weber, K. Bellafrouh, C. Daul, and H. U. Güdel, J. Chem. Phys. **104**, 7624 (1996).
[34] C. Daul, Int. J. Quantum Chem. **52**, 867 (1994).
[35] C. A. Daul, K. G. Doclo, and A. C. Stückl, *Recent Advances in Density Functional Methods, Part II*, edited by Delano Chong (World Scientific, Singapore, 1997).
[36] Pollak, A. Rosa, and E. J. Baerends, J. Am. Chem. Soc. **119**, 7324 (1997).
[37] V. Luaña, G. Fernández Rodrigo, E. Francisco, L. Pueyo, and M. Bermejo, J. Solid State Chem. **66**, 263 (1987).
[38] T. Ziegler, A. Rauk, and E. J. Baerends, Theor. Chim. Acta **43**, 261 (1977).
[39] (a) H. Johansen, Mol. Phys. **49**, 1209 (1983); (b) Chem. Phys. Lett. **156**, 592 (1989).
[40] A. C. Stuckl, C. A. Daul, and H. U. Güdel, J. Chem. Phys. **107**, 4606 (1997).
[41] S. H. Vosko, L. Wild, and M. Nusair, Can. J. Phys. **58**, 1200 (1980).
[42] A. D. Becke, Phys. Rev. A **38**, 3089 (1988).

[43] (a) J. P. Perdew, Phys. Rev. B **33**, 8822 (1986); (b) **34**, 7406 (1986).
[44] T. Ziegler, A. Rauk, and E. J. Baerends, Chem. Phys. **16**, 209 (1976).
[45] DIPOLE version 1.1, Theoretical Chemistry Department, Vrije Universiteit, Amsterdam.
[46] M. F. Reid, J. Phys. Chem. Solids **49**, 185 (1988).
[47] L. Noddleman, J. Chem. Phys. **64**, 2343 (1976).
[48] R. S. Berry, S. A. Rice, and J. Ross, *Physical Chemistry* (Wiley, New York, 1980), p. 815.
[49] M. Born and K. Huang, *Dynamical Theory of Crystal Lattices* (Oxford University Press, London, 1954), p. 60.
[50] S. Sugano and R. G. Shulman, Phys. Rev. B **130**, 517 (1963).
[51] J. A. Aramburu and M. Moreno, Phys. Rev. B **56**, 604 (1997).
[52] F. Rodríguez and M. Moreno, J. Chem. Phys. **84**, 692 (1986).
[53] S. J. Duclos, Y. K. Vohra, and A. L. Ruoff, Phys. Rev. B **41**, 5372 (1990).
[54] M. Moreno, J. A. Aramburu, and M. T. Barriuso, Phys. Rev. B **56**, 14423 (1997).
[55] Y. Toyozawa and M. Inoue, J. Phys. Soc. Jpn. **21**, 1663 (1966).
[56] M. C. Marco de Lucas, thesis, Universidad de Cantabria, 1992.
[57] H. Adachi, S. Shiokawa, M. Tsukada, C. Satoko, and S. Sugano, J. Phys. Soc. Jpn. **47**, 1528 (1979).
[58] H. Nakai, H. Morita, and H. Nakatsuji, J. Phys. Chem. **100**, 15753 (1996).
[59] J. Simonetti and D. S. McClure, J. Chem. Phys. **71**, 793 (1979).
[60] K. Wissing, J. A. Aramburu, M. T. Barriuso, and M. Moreno, Solid State Commun. (in press).
[61] M. Atanasov, H. Adamsky, and K. Eifert, J. Solid State Chem. **128**, 1 (1997).
[62] I. Cabria, M. T. Barriuso, J. A. Aramburu, and M. Moreno, Int. J. Quantum Chem. **61**, 627 (1997).